Stoichiometric Effects on Bulk Stress Relaxation to Enhance Reprocessability in Covalent Adaptable Networks

Jaehyun Cho[a], Santanu Ghosh[c], Mridula Nandi[c], Heejoon Jeon[b], Liang Yue[d], H. Jerry Qi[d], M.G. Finn[c], Blair Brettmann[a,b]

[a] School of Chemical and Biomolecular Engineering, Georgia Institute of Technology, Atlanta, GA, USA

[b] School of Materials Science and Engineering, Georgia Institute of Technology, Atlanta, GA, USA

[c] School of Chemistry and Biochemistry, Georgia Institute of Technology, Atlanta, GA, USA

[d] The George W. Woodruff School of Mechanical Engineering, Georgia Institute of Technology, Atlanta, GA, USA

Determining Functionality of Jeffamine and polyethylene imine

Attenuated total reflectance-Fourier transform infrared spectroscopy (ATR-FTIR) was used to measure the empirical reactivity of each functional group on the amine monomers. The spectra for each monomer was collected (Figure S1) and both Jeffamine (Figure S2-S3) and PEI (Figure S4) were individually reacted with TMPTA to estimate the empirical functionality. Peaks for analysis were chosen based on the spectra of the individual materials (Figure S1). The TMPTA exhibits C=C bonds at three different positions: 1637 cm^{-1}, 1407 cm^{-1}, and 807 cm^{-1}[1–4]. For the amines, the absorbance peaks of amines are observed in both Jeffamine and PEI at 3000-3500 cm^{-1}, 1500-1650 cm^{-1}, and 767 cm^{-1}[3]. To determine the empirical functionality, the mixing ratio was achieved by gradually increasing the amount of the reacting amine species relative to a fixed amount of acrylate. As the Aza-Michael addition reaction progresses, the disappearance of acrylate peaks were tracked and the FTIR spectra were normalized to the C=O bond position, which is inactive in the addition reaction, facilitating quantitative comparison of remaining peak intensities.

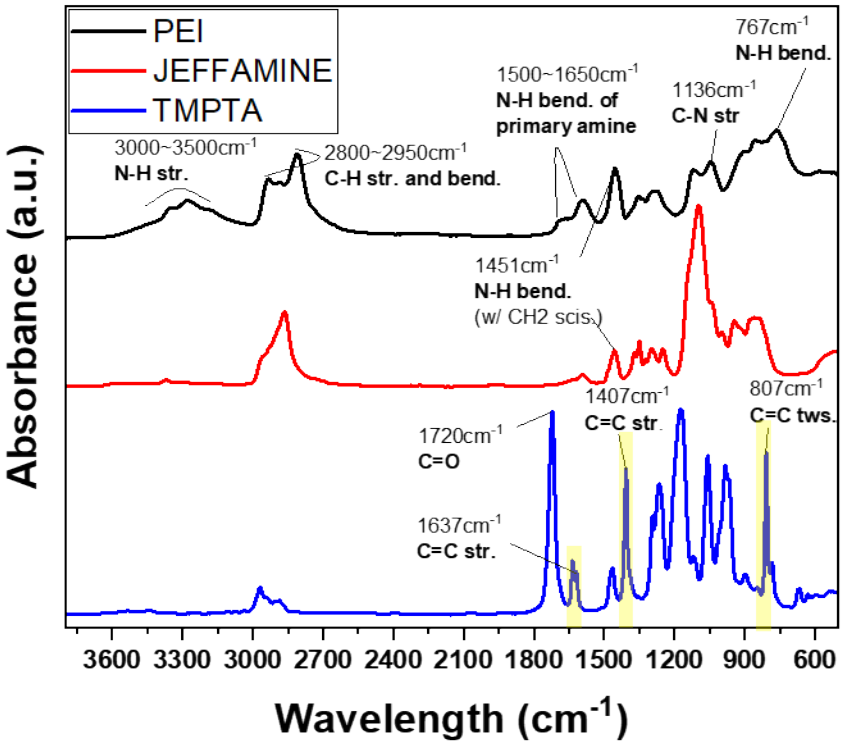

Fig. S1. FT-IR analysis for each monomer: PEI, Jeffamine, and TMPTA.

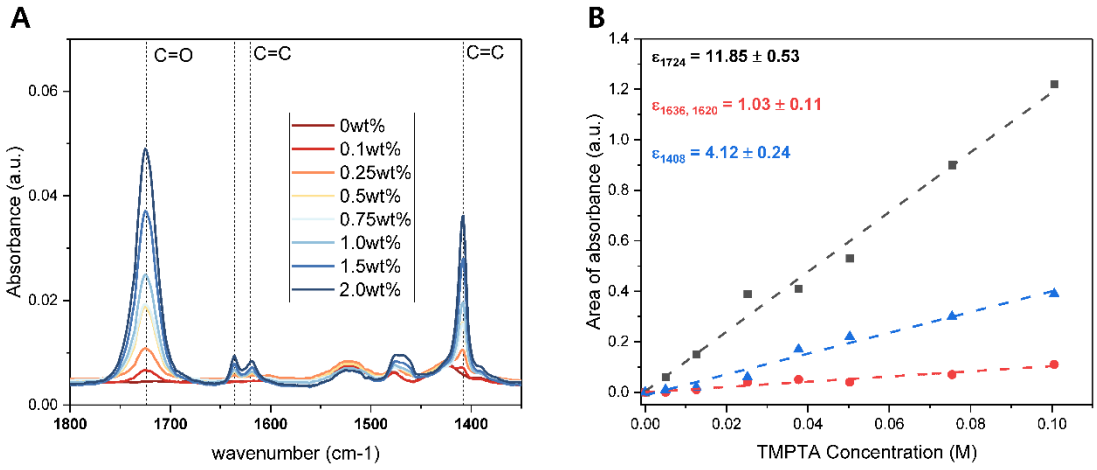

Fig. S2. ATR-FTIR for solutions of TMPTA in DMF with varying weight % of TMPTA (A) and measured absorption coefficients (ε), the slope of the linear regression) for characteristic ATR-FTIR signals of TMPTA (B). Error is the standard error from the linear regression.

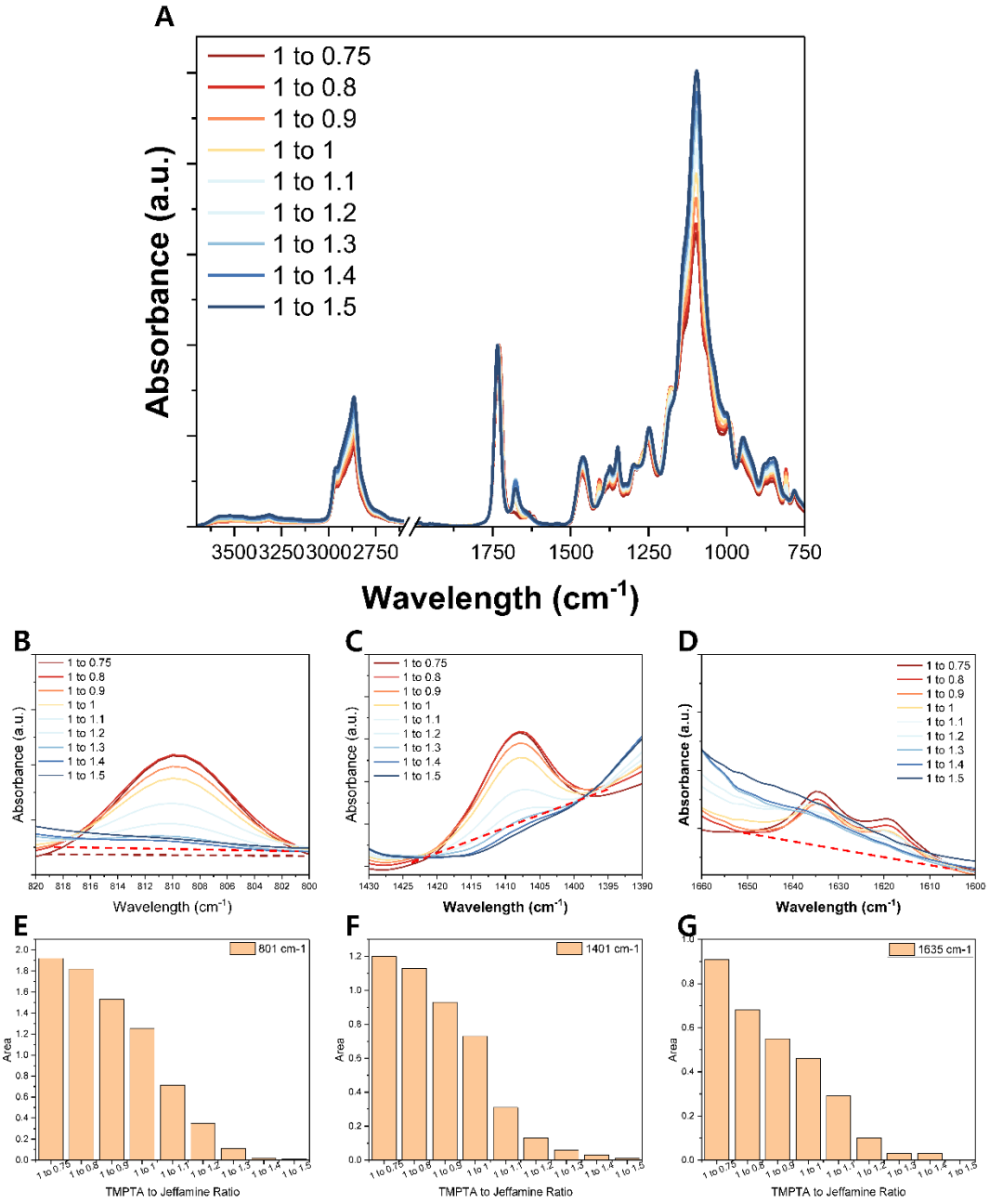

Fig. S3. ATR-FTIR analysis to determine the functionality of Jeffamine (*f* was determined to 2.2 based on this experiment). Full range FTIR spectra (A), enlarged view from 820cm^{-1} to 795cm^{-1} (B), from 1440cm^{-1} to 1380cm^{-1} (C), and from 1660cm^{-1} to 1600cm^{-1} (D). The area under each curve was estimated using the baselines, shown as dashed lines in the graph. The area under the curve corresponds to each composition is shown for 820cm^{-1} to 795cm^{-1} (E), from 1440cm^{-1} to 1380cm^{-1} (F), and from 1660cm^{-1} to 1600cm^{-1} (G). These spectra were normalized to keep the carbonyl peak intensity (1729-1735 cm^{-1}) constant.

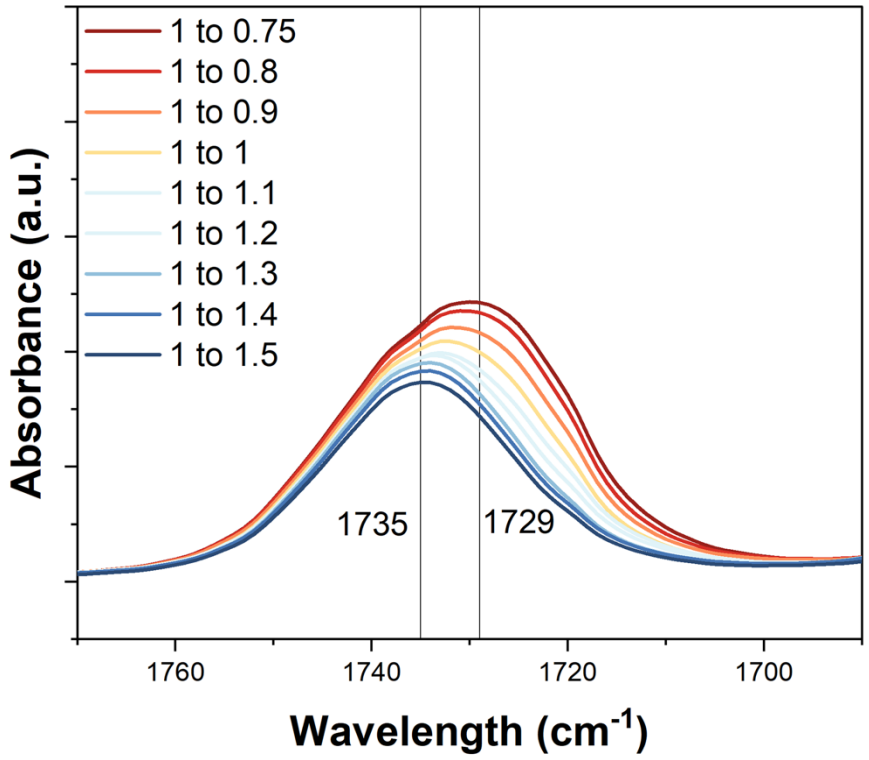

Fig. S4. Carbonyl stretching band from ATR-FTIR of the samples shown in Fig. S2 without intensity normalization.

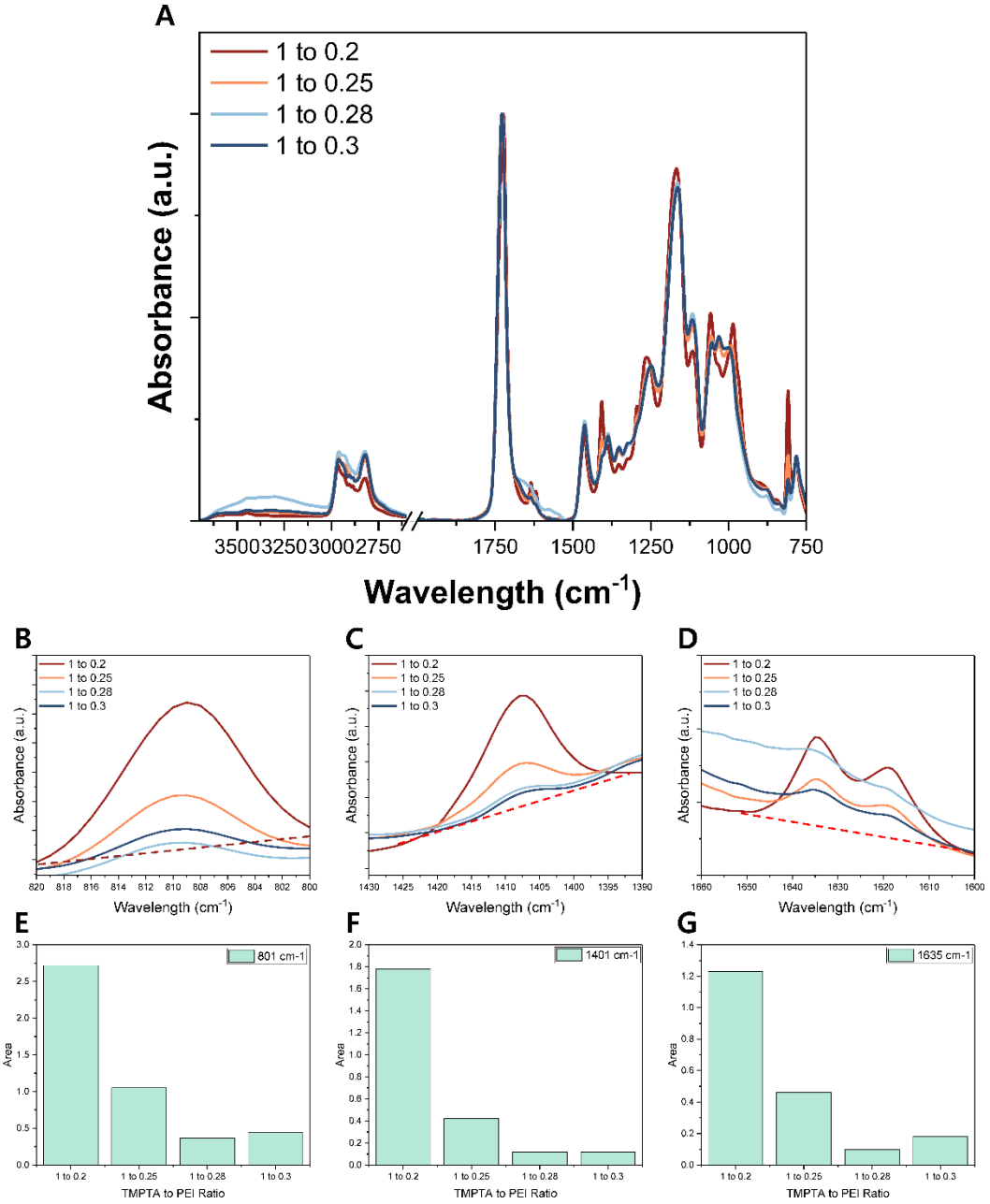

Fig. S5. ATR-FTIR analysis to determine the functionality of polyethylene imine (*f* was determined to 13 based on this experiment). Full range FTIR spectrum measurement (A), enlarged view from 825cm^{-1} to 790cm^{-1} (B), from 1440cm^{-1} to 1380cm^{-1} (C), and from 1660cm^{-1} to 1600cm^{-1} (D). The area under each curve was estimated using the baselines, shown as dashed lines in the graph. The area under the curve corresponds to each composition is shown for 825cm^{-1} to 790cm^{-1} (E), from 1440cm^{-1} to 1380cm^{-1} (F), and from 1660cm^{-1} to 1600cm^{-1} (G).

^{1}H NMR was also employed to measure the stoichiometry of Jeffamine reactivity.

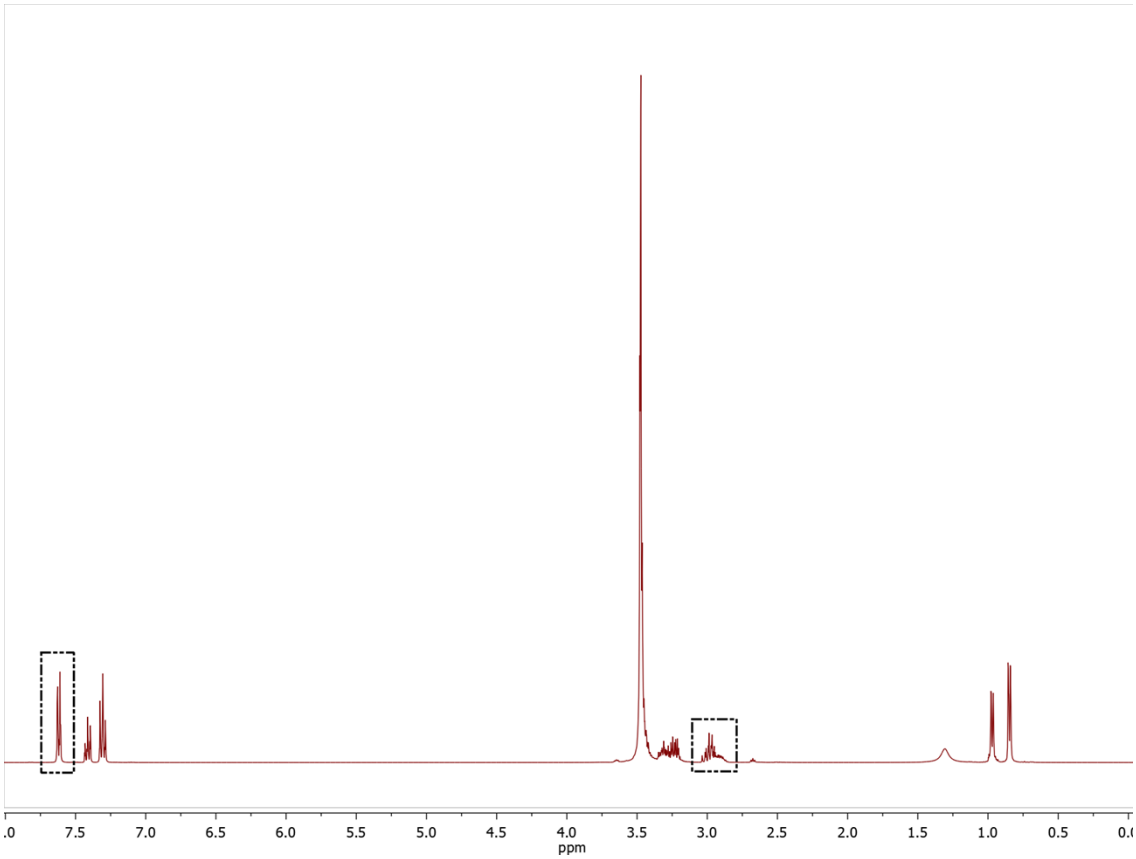

Fig. S6. ^{1}H NMR of Jeffamine in $CDCl_3$ with benzophenone as an internal standard.

Using the integral values from the NMR spectra (Fig. S6), initial mass of Jeffamine and benzophenone taken, and the molecular weight of benzophenone, the AHEW was found to be in the range of 310 – 330 g/mol. The experiment was run twice with different amounts of Jeffamine and benzophenone and the functionality was found to be 1.85 and 1.9 for the two samples, (See Materials and Methods section for experimental details).

Raw data from stress relaxation measurements

The normalized stress relaxation modulus of all compositions was measured from 150°C to 180°C. Different compositions are represented by solid, dashed, and dotted lines, while the color changes from dark red to orange-yellow to represent the test temperature. A horizonal line is drawn at a relaxation modulus of 1/e, which was used to extract the characteristic time.

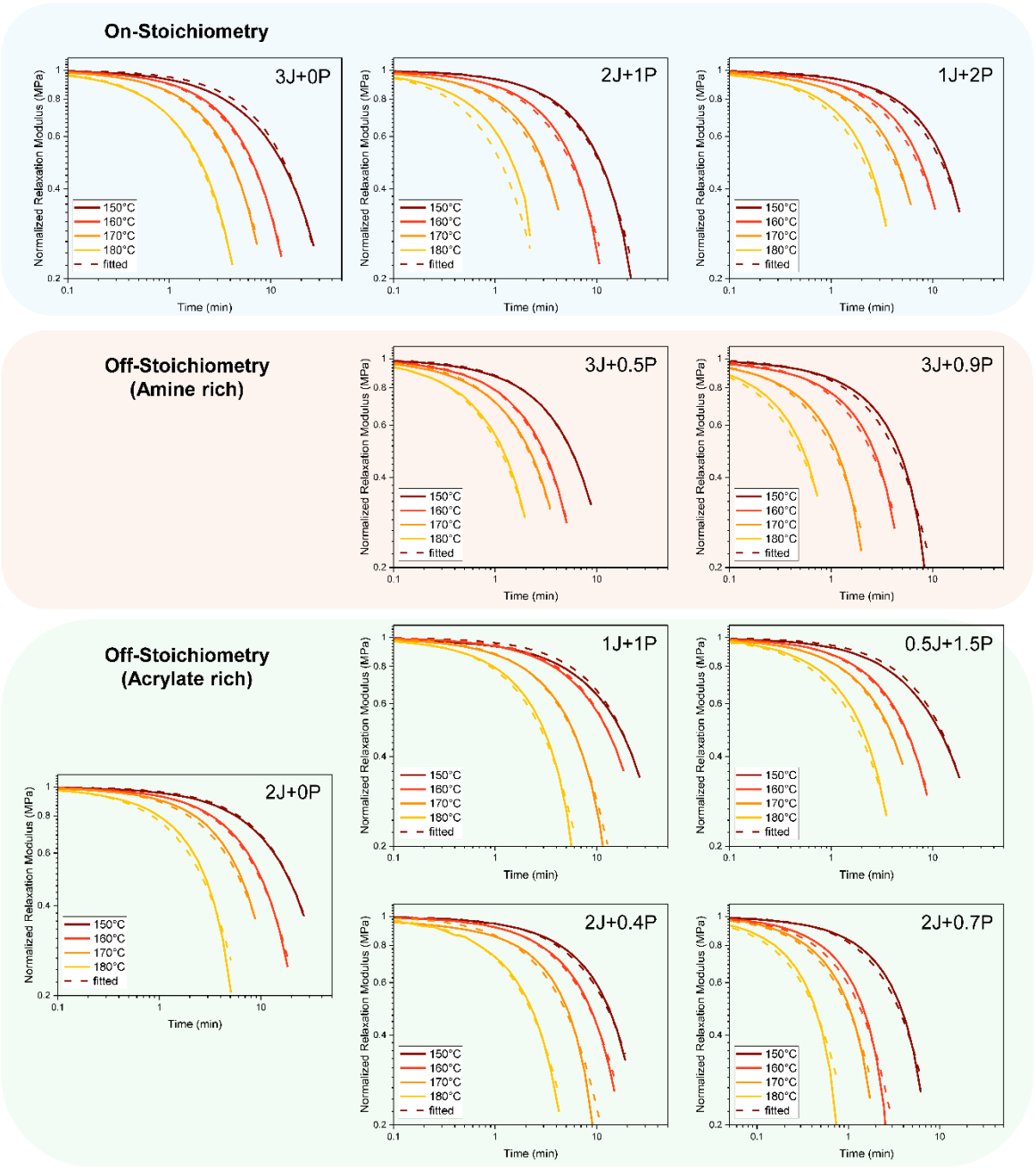

Fig. S7. DMA stress relaxation measurement raw data for 'on-stoichiometry' (blue shade, top), the excess amine case (red shade, middle), and for the excess acrylate cases (green shade, bottom) with concurrently changing Jeffamine to PEI ratio and fixed Jeffamine and changing PEI ratio. The dashed line is single Maxwell model fitting, indicating a good fit to experimental data.

Activation energy

The activation energy was determined from the slope of a line fit to the data of natural log of the characteristic time vs. 1000/temperature. The R^2 value of each linear fit is provided and the uncertainty reported for the activation energy is the standard error of the slope from linear regression.

Table S1: Activation energy values and R^2 from the linear fits for all compositions studied.

Composition Category		Sample Code	Ea (KJ/mol)	R-square
On-Stoichiometry		3J+0P	98±6	0.995
		2J+1P	106±8	0.988
		1J+2P	92±5	0.996
Off-Stoichiometry	**Excess Amine**	3J+0.5P	84±8	0.983
		3J+0.9P	98±13	0.961
	Excess Acrylate (decreasing Jeffamine and increasing PEI)	2J+0P	113±16	0.961
		1J+1P	89±11	0.971
		0.5J+1.5P	100±16	0.924
	Excess Acrylate (fixed Jeffamine and increasing PEI)	2J+0.4P	104±17	0.935
		2J+0.7P	113±29	0.874

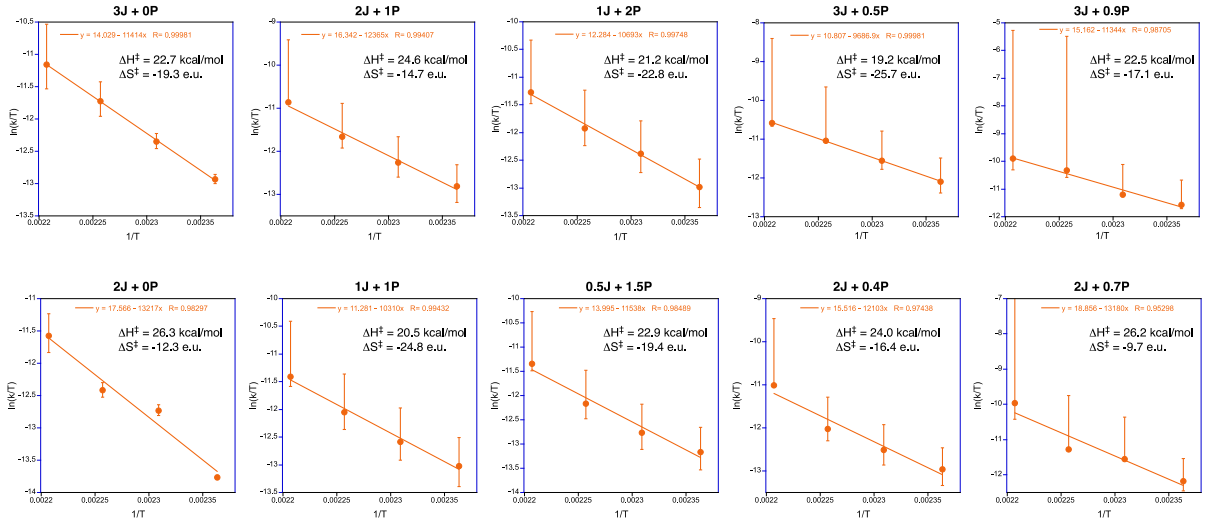

Fig. S8. Eyring plots for all samples.

Model compound reactions

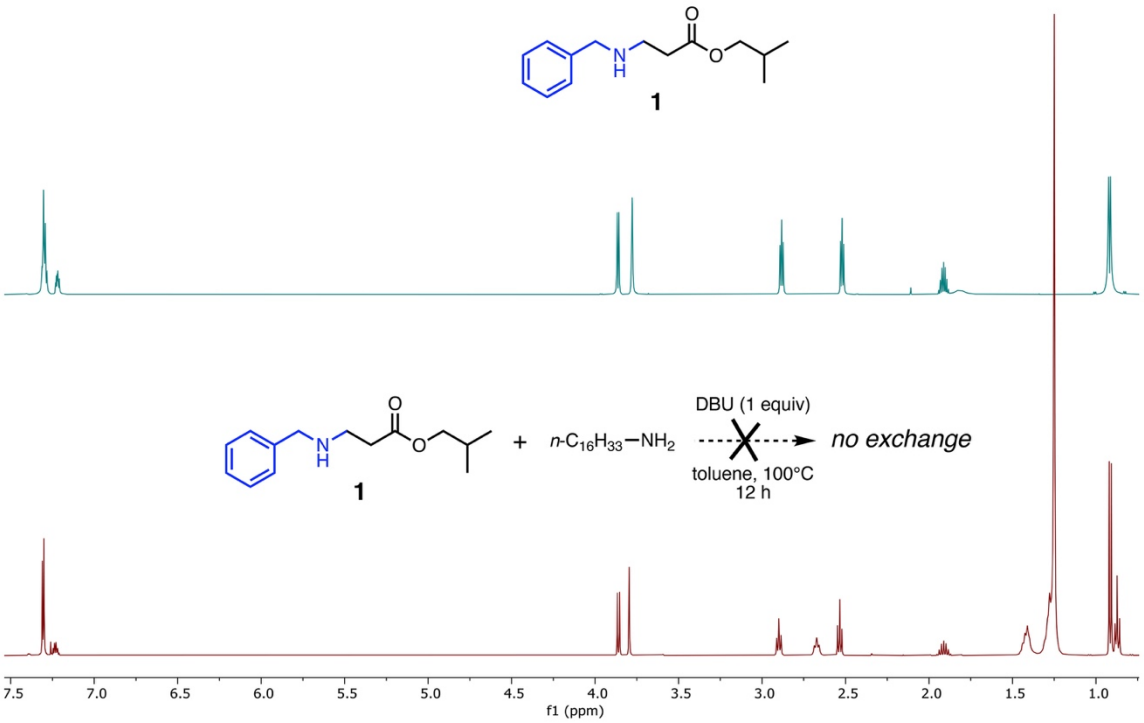

Fig. S9A. ^{1}H NMR spectra ($CDCl_3$) of model reaction of isobutyl acrylate adduct with another amine

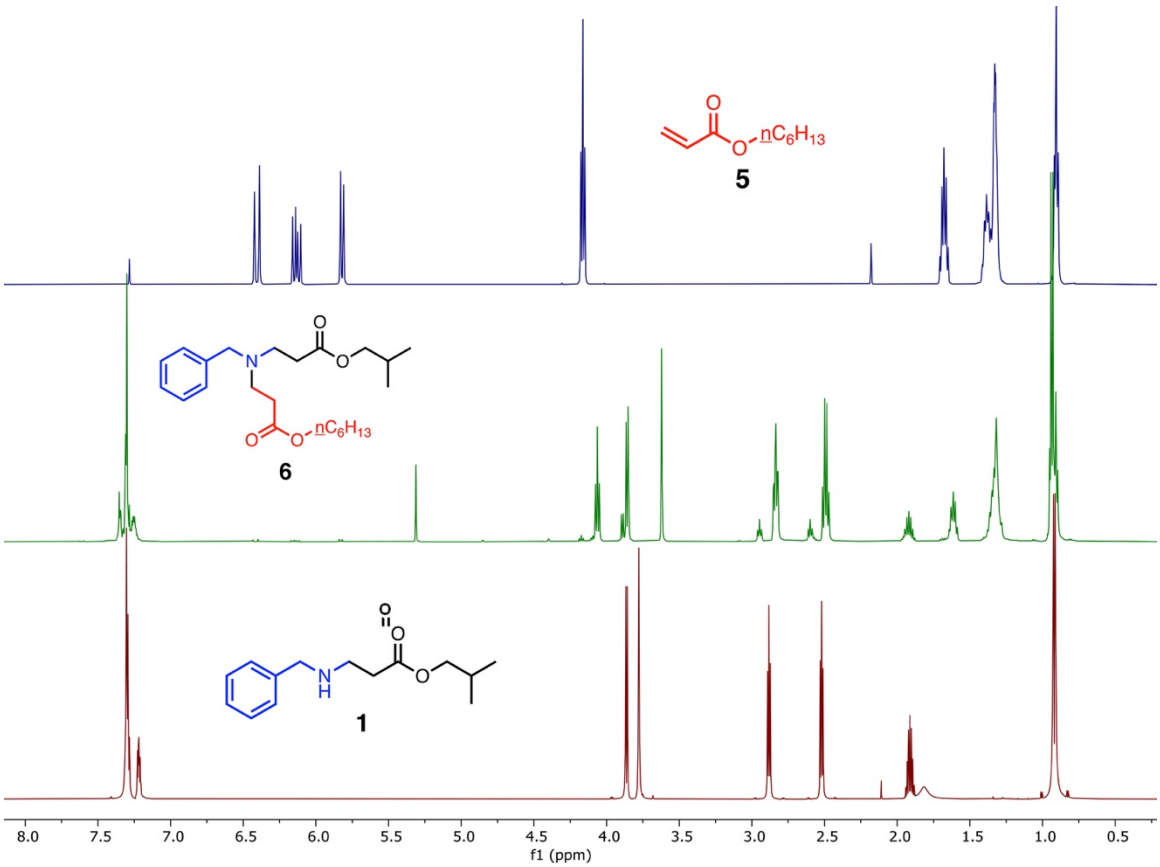

Fig. S9B. ^{1}H NMR spectra (CDCl3) comparison of model reaction

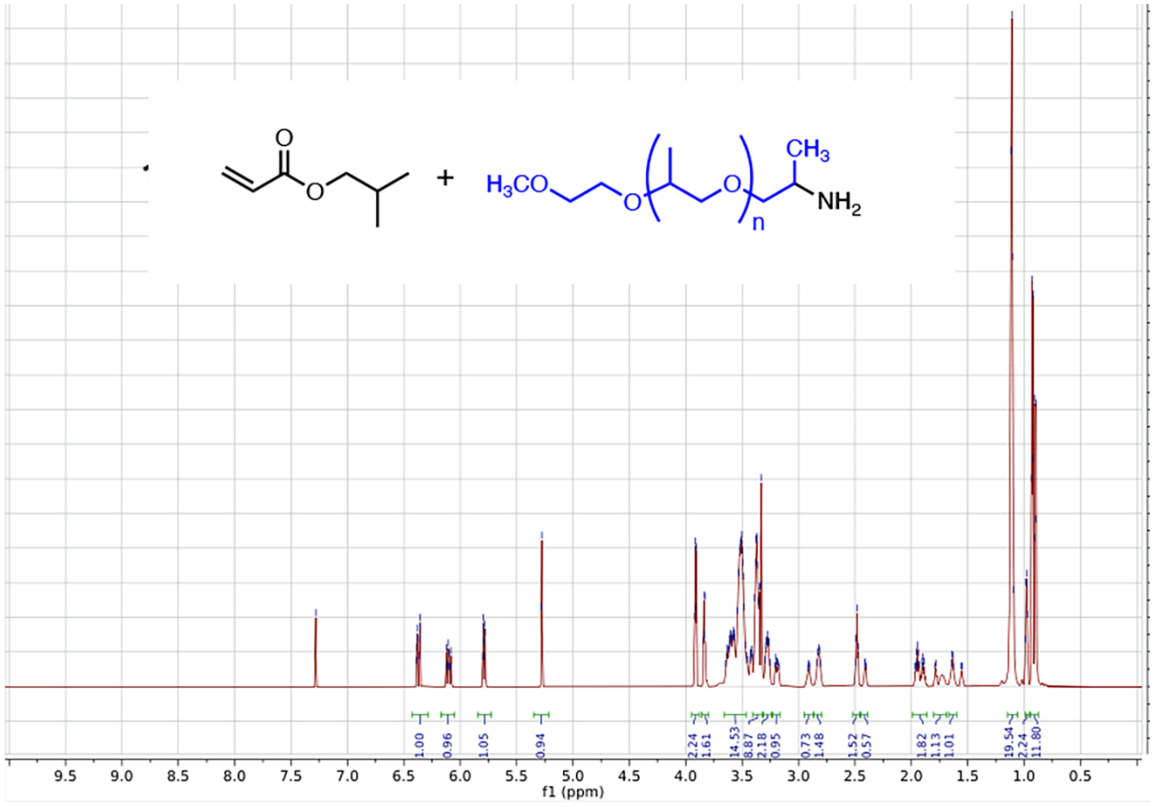

Fig. S9C. ^{1}H NMR spectra (CDCl3) of a mixture of isobutyl acrylate and polypropylene glycol

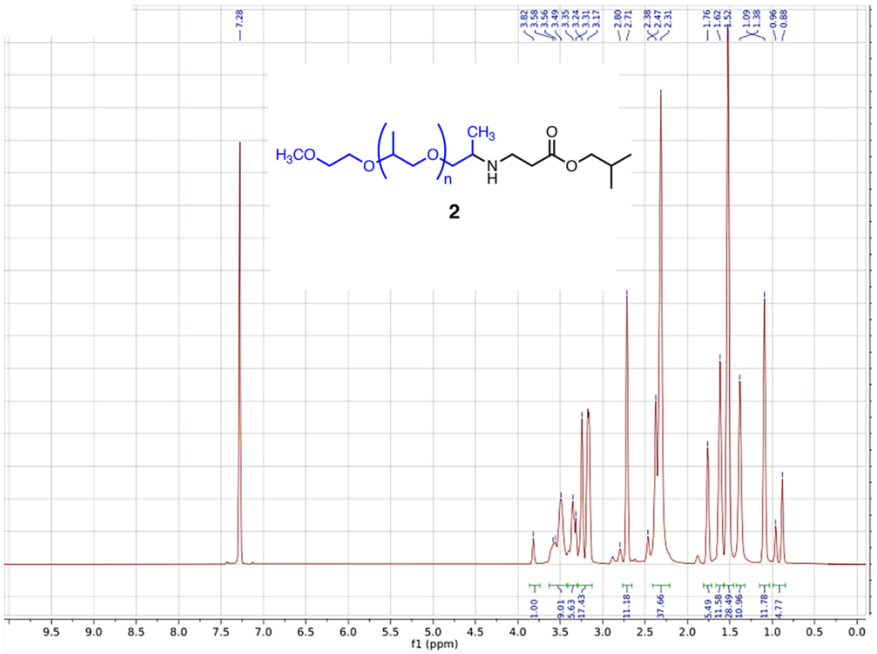

Fig. S9D. ^{1}H NMR spectra (CDCl3) for the adduct formed from isobutyl acrylate and polypropylene glycol

FTIR analysis for possible chemical change over thermal reprocessing of samples

ATR-FTIR analysis was conducted to identify any possible chemical degradation with thermal reprocessing. Spectra are not normalized due to possible intensity changes of the peak at 1724cm^{-1}, C=O peak.

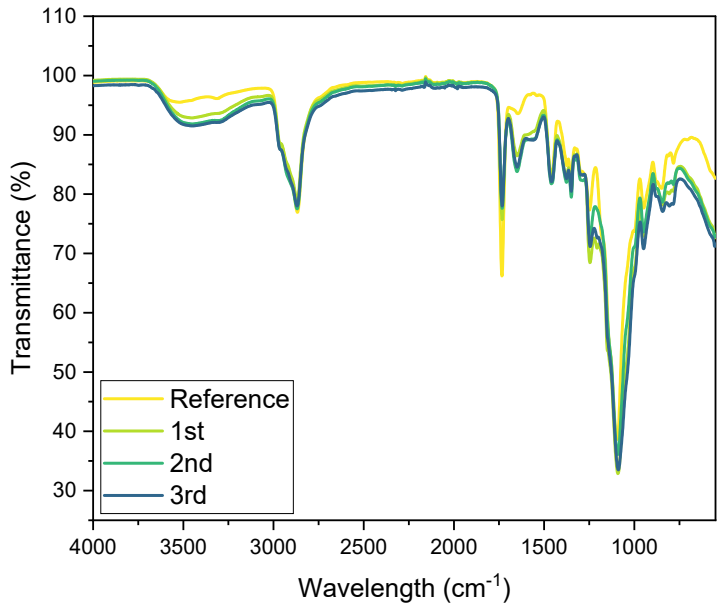

Fig. S10. FTIR spectra of samples cured in oven (Reference means the on stoichiometric 3J+0P sample), and 1st to 3rd times of thermal reprocessing.

Raw data from reprocessing stress relaxation and plateau modulus measurements

DMA analysis was conducted to investigate the effect of thermal reprocessing on the stress relaxation behavior and structural integrity. Figures S9-A and S9-B display the stress relaxation measurements conducted at 160°C, while Figures S9-C and S9-D present the storage modulus with ramping temperatures and corresponding tan delta curves.

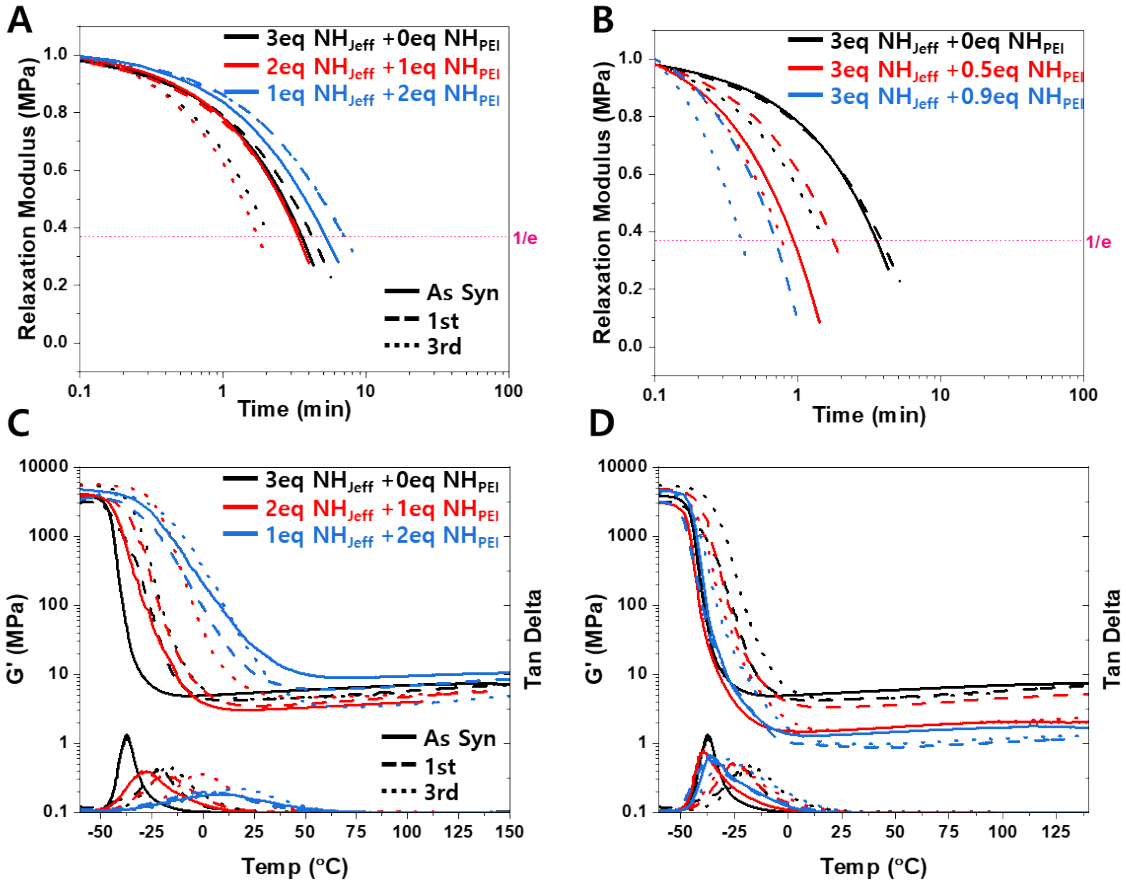

Fig. S11. DMA stress relaxation measurement raw data for 'on-stoichiometry' (A), excess amine (B) and DMA storage modulus measurement in temperature ramping mode for 'on-stoichiometry' (C), excess amine (D) with up to 3 times thermal reprocessing for each case.

Bulk properties of CANs

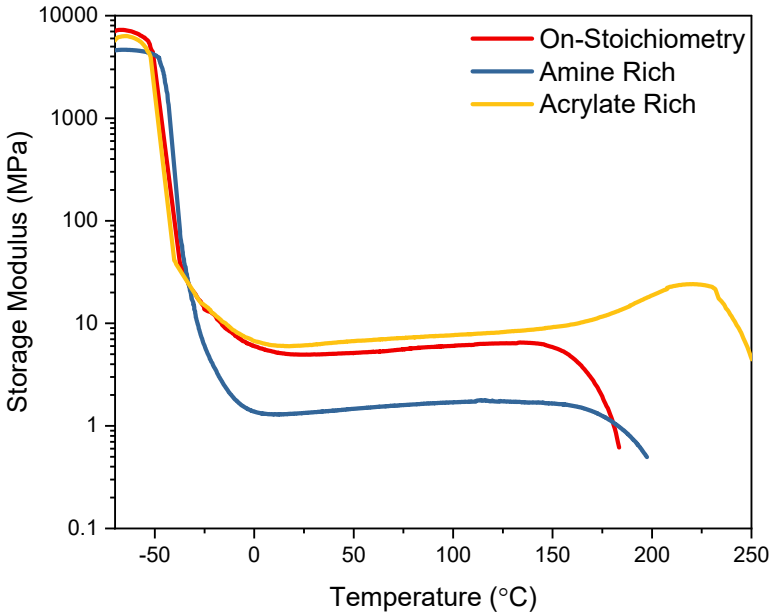

Fig. S12. Storage modulus profiles of different stoichiometric variation in samples measured using DMA.

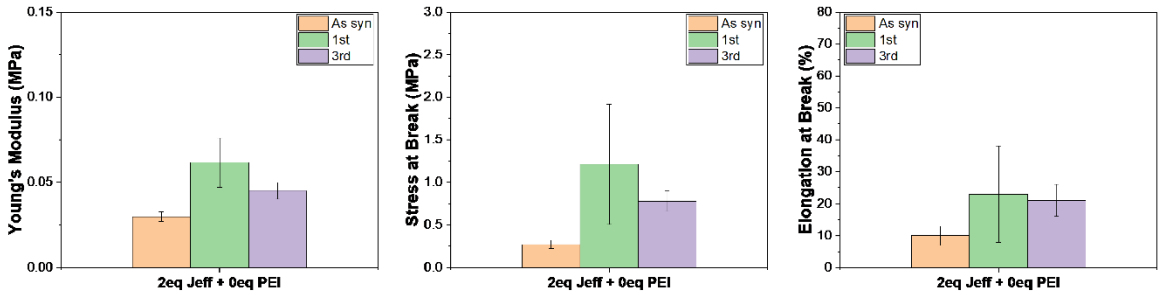

Fig. S13. Tensile measurements of off-stoichiometry excess acrylate cases for three reprocessing cycles.

References

1 A. O. Konuray, X. Fernández-Francos, À. Serra and X. Ramis, *European Polymer Journal*, 2016, **84**, 256–267.

2 T. Wen-Dong, H. Guang-Jian, H. Wei-Tao, Z. Xin-Liang, C. Xian-Wu and Y. Xiao-Chun, *CrystEngComm*, 2021, **23**, 864–875.

3 K. Grenda, A. Idström, L. Evenäs, M. Persson, K. Holmberg and R. Bordes, *Journal of Applied Polymer Science*, 2022, **139**, 51657.

4 M. Zhu, Z. Cao, H. Zhou, Y. Xie, G. Li, N. Wang, Y. Liu, L. He and X. Qu, *RSC Adv.*, 2020, **10**, 10277–10284.